SCIENCE

AMERICAN ASSOCIATION FOR THE ADVANCEMENT OF SCIENCE

24 December 1976, Volume 194, No. 4272

COVER

First nuclear magnetic resonance image of a tumor in a live animal. The image was achieved by FONAR spectroscopy. The tumor, an Ehrlich ascites solid neoplasm of the anterior chest wall, is the orange-pink and red region at the bottom of the image. In the normal mouse the thoracic region is blue. See page 1430. [Raymond Damadian *et al.*, State University of New York at Brooklyn]

Reprinted from
24 December 1976, Volume 194, pp. 1430-1432

SCIENCE

Field Focusing Nuclear Magnetic Resonance (FONAR): Visualization of a Tumor in a Live Animal

Abstract. *A nuclear magnetic resonance (NMR) image of a tumor in a live animal is reported. The field focusing NMR method or* FONAR *process that now achieves the tumor outline is described.*

Since the introduction of the nuclear resonance technique for detecting cancer by Damadian (*1*), many other investigators (*2, 3*) have extended the observation, including Weisman *et al.* who demonstrated its utility in vivo by detecting a tumor on the tail of a live mouse (*3*). The method of Damadian, originally conceived for the detection of internal neoplasms in humans, achieved its objective by focusing the nuclear magnetic resonance (NMR) signal within the interior of the live host. The focused NMR signal was thereby externally directed to any internal location in the live subject for data acquisition. The focusing NMR technique (called FONAR) was developed in 1972 (*4*).

FONAR should be distinguished from various nonfocusing methods that have appeared since. A promising modification of the projection analysis methods is the Fourier transform imaging technique by Kumar, Welti, and Ernst (*5*). Focusing NMR permits the operator to externally direct the NMR spot to the anatomic site of interest for firsthand inspection of the signal characteristics at a suspicious locus. Furthermore, field focusing allows the NMR signal behavior of each anatomic region to be continuously monitored during the data acquisition phase of the FONAR imaging process.

In principle, focusing NMR is achieved by field regulation of the spatial boundaries of a signal-producing region inside a sample. This is accomplished by shaping the magnetic fields (H_0 and H_1) across the entire sample so as to construct a small resonant window within the sample, such that the ratio of the spin moment of the nucleus to its gyric moment is everywhere satisfied by the static and time varying H fields and is everywhere dissatisfied beyond its boundaries. In practice, both the static H_0 field and the inductive component of the radio frequency (rf) field (H_1) are shaped. The

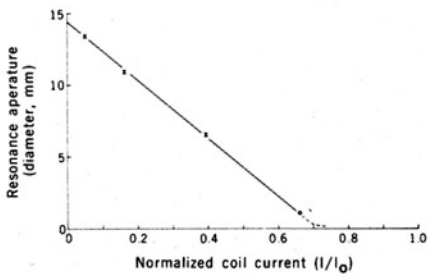

Fig. 1. Resonance aperture versus coil current. The o point shown is the extrapolated normalized current value for a 1-mm aperture.

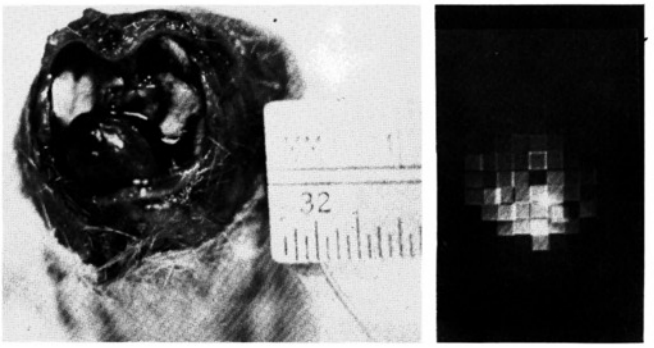

Fig. 2. Cross-sectional video FONAR image of a live mouse, obtained with a 3-mm exploring spot. At the left is a photograph of the anatomical section for comparison. The heart is anterior in the photo, and the lungs, seen as collapsed white structures, fill the remainder of the thorax. The most intense proton signal in the FONAR image occurs in the region of the blood-filled heart. The dark fields in the upper half of the photo were generated by the hydrogen-poor air-filled lungs. The television raster is seen coursing through the image. Overlap artifacts appear in the image as bright, vertical and horizontal lines and are due to imperfect positioning of adjacent mapping squares.

system of field correction coils for shaping H_0 was determined from the series solution of the Laplace equation in spherical coordinates,

$$\psi(r, \theta, \phi) = \sum_{m,n} \left(\frac{r}{a}\right)^n P_n^m(\cos\theta) [A_{mn}\cos m\phi + B_{mn}\sin m\phi]$$

where ψ is the scalar potential; r, θ, and ϕ are the spherical coordinates, with P_n^m the associated Legendre polynomials (*6*). The axial magnetic induction B_z of the coil system is then computed from the scalar potential using $B = -\nabla\psi$ for the case where the curl of B is taken as zero outside the surface enclosed by the coils. The field B_z can then be expanded in the derivatives of ψ. A linear combination of terms of the B_z expansion provides the H_0 field-regulating system that, together with H_1 shaping, controls the resonating volume, or resonance aperture in three dimensions (*7*).

We estimated the size of the resonance aperture achieved by our focusing technique as follows. A sample tube 19 mm (control) in inside diameter and filled with $NiCl_2$-doped water was placed in the NMR probe. The height of the free induction decay (FID) of the hydrogen signal after a 90° pulse was determined for a series of currents in the focusing coils and recorded. Phase adjustment was required for a maximum FID at each new current setting. The experiment was then repeated for a 13.5-mm (inside diameter) sample tube (experimental) and a plot was made of the ratio of signal intensities (FID amplitudes) generated by the control and experimental samples at each current setting. The current at which this intensity ratio attained a value of unity was taken as the current at which the diameter of the signal-producing region within the large tube equaled the inside diameter of the smaller tube. The coil current at the unity point, therefore, specified the current needed to produce a resonance aperture of diameter equal to the inside diameter of the experimental tube. At lesser currents, the resonance aperture exceeded the diameter of the smaller tube, the larger tube therefore generated more signal than the smaller, and the intensity ratio exceeded 1. The coil current required to achieve a unity intensity ratio for an 11- and 6.5-mm tube was also determined. A plot of tube diameters as a function of the normalized coil current (Fig. 1) generated an extrapolated estimate of the current required to achieve the 1-mm resonance aperture used in animal imaging.

The scan for developing the FONAR image moves the resonance aperture through an anatomic cross section, either by moving the animal with respect to the aperture or by moving the aperture, with the animal being held stationary. The method provides visible proton signal, without signal processing, from scanning apertures that are approximately spherical and estimated at slightly less than 1 mm.

The televised output is a stored video record of proton signal intensities (FID amplitudes) at various xy coordinates, generated by the resonance aperture as it was swept through a cross section of the animal's torso. While it was not so applied in this instance, the technique is readily adaptable to constructing images from T_1 (spin lattice relaxation) or T_2 (spin-spin relaxation) data taken at each of the FONAR loci of the scan. The Freeman-Hill method of progressive saturation (*8*) for obtaining T_1 is well suited to this purpose.

Video FONAR images were obtained in a CSCC (Canada Superconductor) superconducting magnet with the use of a SEIMCO (New Kensington, Pennsylvania) model RD variable frequency pulse spectrometer operating at 10 Mhz. The animal was successfully immobilized in the probe for 4 hours with 0.2 ml of valium (5 mg/ml) injected intraperitoneally. Figure 2 is a direct televised image of a section through the thorax of a live mouse at the level of the mediastinum. A photo of the postmortem anatomic section at the level of the cross-sectional image is in the left of the figure for direct comparison. The heart is anterior in the photo and the lungs, seen as collapsed white structures, fill the remainder of the thorax. A 3-mm scanning aperture was used. The most intense proton signal occurs in the region of the blood-filled heart. The signal-deficient dark fields in the upper half of the photo were generated by the proton-poor air-filled lungs. The television raster is seen coursing through the image. Overlap artifacts, appearing in the image as bright vertical and horizontal lines, are due to imperfect positioning of adjacent mapping squares.

Shown on the cover of this issue is a color video FONAR image of a cross section through the upper thorax (above the mediastinum) of a mouse that had a solid Ehrlich ascites tumor surgically implanted in the anterior chest wall. Each colored area designates a different range of signal amplitude. The anterior orange-pink and red region (at the bottom of the image), not present in normal control mice and indicative of a signal-producing mass, corresponds with the location of the tumor. The resolving limitation of a 1-mm scanning aperture in a 13-mm sample (thorax diameter) overestimates the tumor size partially obscuring the underlying lung fields. In the normal animal (not shown), the anterior half of the thorax appears as a blue signal-poor region representing the lung cavities. Having originally introduced the NMR method chiefly for the purpose of noninvasively detecting internal tumors in humans, we have succeeded in obtaining the first images of a tumor in a live animal.

RAYMOND DAMADIAN
LAWRENCE MINKOFF
MICHAEL GOLDSMITH
MICHAEL STANFORD
JASON KOUTCHER

Biophysical Laboratory, State University of New York at Brooklyn, 450 Clarkson Avenue, Brooklyn, New York 11203

References and Notes

1. R. Damadian, *Science* **171**, 1151 (1971).
2. H. E. Frey, R. R. Knispel, J. Kruuv, A. R. Sharp, R. T. Thompson, M. M. Pintar, *J. Natl. Cancer Inst.* **49**, 903 (1972); G. P. Raaphorst, J. Kruuv, H. Frey, in *The Nuclear Resonance Effect in Cancer*, R. Damadian, Ed. (Pacific Press, New York, in press); C. F. Hazlewood, D. C. Chang, D. Medina, G. Cleveland, B. L. Nichols, *Proc. Natl. Acad. Sci. U.S.A.* **69**, 1478 (1972); G. L. Cottam, A. Vasek, D. Lusted, *Res. Commun. Chem. Pathol. Pharmacol.* **4**, 495 (1972); R. G. Parrish, R. J. Kurland, W. W. Janese, L. Bakey, *ibid.* **183**, 438 (1973); D. P. Hollis, L. A. Saryan, H. P. Morris, *Johns Hopkins Med. J.* **131**, 441 (1972); D. P. Hollis, J. S. Economou, L. C. Parks, J. C. Eggleston, L. A. Saryan, J. L. Czeisler, *Cancer Res.* **33**, 2156 (1973); R. A. Floyd, J. S. Leigh, B. Chance, M. Miko, *ibid.* **34**, 89 (1974); I. C. Kiricuta, D. Demco, V. Simplaceanu, *Arch. Geschwulstforsch.* **42**, 226 (1973); R. E. Block, *FEBS Lett.* **34**, 109 (1973); W. R. Inch, J. A. McCredie, R. R. Knispel, R. T. Thompson, M. M. Pintar, *J. Natl. Cancer Inst.* **52**, 353 (1974); W. Bovee, P. Huisman, J. Smidt, *ibid.*, p. 595; L. A. Saryan, D. P. Hollis, J. S. Economou, J. C. Eggleston, *ibid.*, p. 599; C. F. Hazlewood, G. Cleveland, D. Medina, *ibid.*, p. 1849; R. E. Block and G. P. Maxwell, *J. Magn. Reson.* **14**, 329 (1974); B. M. Fung, *Biochim. Biophys. Acta* **362**, 209 (1974); S. Ratkovic and C. Rusov, *Period. Biol.* **76**, 19 (1974); S. S. Ranade, S. S. Shah, K. S. Korgaonkar, C. V. Talwalkar, S. R. Kasturi, paper presented at the Fifth International Symposium on Magnetic Resonance, Bombay, India, 14 to 18 January 1974; C. F. Hazlewood, in *The Nuclear Resonance Effect in Cancer*, R. Damadian, Ed. (Pacific Press, New York, in press); I. D. Weisman, L. H. Bennett, L. R. Maxwell, in *ibid.*; W. Bovee and J. Smidt, in *ibid.*; N. Iijima, S. Saitoo, Y. Yoshida, N. Fujii, T. Koike, K. Osanai, K. Hirose, in *ibid.*; M. M. Pintar, in *ibid.*; S. Ratkovic and C. Rusov, in *ibid.*; S. S. Ranade, in *ibid.*; R. E. Gordon, J. R. Singer, L. Crooks, in *ibid.*; Z. Abe and K. Tanaka, in *ibid.*
3. I. D. Weisman, L. H. Bennett, L. R. Maxwell, M. W. Woods, D. Burk, *Science* **178**, 1288 (1972).
4. R. Damadian, U.S. Patent 3,789,832, filed 17 March 1972.
5. A. Kumar, D. Welti, R. R. Ernst, *Naturwissenschaften* **62**, 34 (1975).
6. P. M. Morse and H. Feshbach, in *Methods of Theoretical Physics II*, (McGraw-Hill, New York, 1953), p. 1265.
7. R. Damadian, in *The Nuclear Resonance Effect in Cancer*, R. Damadian, Ed. (Pacific Press, New York, in press).
8. R. Freeman and H. D. Hill, *J. Chem. Phys.* **54**, 3367 (1971).

9. Supported in part by grant R01-CA 14988-06 from the National Institute of Health.

23 July 1976; revised 24 September 1976